Bifurcation analysis of digital force control with nonlinear stiffness

Rudolf R. Toth* and Gabor Stepan*
*Department of Applied Mechanics, Budapest University of Technology and Economics, Budapest, Hungary

Summary. Nonlinear stiffness characteristics appear regularly in engineering applications including in systems with digital feedback. This paper proposes a novel method for bifurcation analysis of sampled systems with continuous nonlinearities and the presented approach is used to predict the characteristics of Hopf bifurcations in the digital force control of a mass and nonlinear spring system.

Introduction

In engineering applications, nonlinear stiffness characteristics often appear due to material properties or simply due to the system geometry. With the widespread use of digital controllers, it is common to encounter dynamical systems characterized by both digital sampling and continuous nonlinearities [1]. In this paper, force control with a sampled linear proportional controller of a mass and nonlinear spring system is investigated using the developed novel approach.

Mechanical model and stability

In this section, the mechanical model of force control with nonlinear stiffness is introduced and the linearized stability is presented [2]. The mechanical model in Fig. 1. represents a manufacturing process with prescribed contact force.

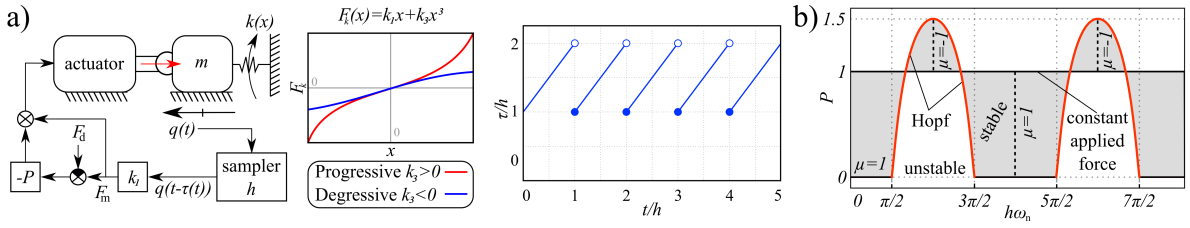

Figure 1: Mechanical model of nonlinear force control, panel a). Stability chart of force control, panel b).

The corresponding nonlinear equation of motion of the controlled body reads

$$\ddot{x}(t) + \omega_n^2 x(t) + \alpha x^3(t) = (1-P)\omega_n^2 x(t-\tau(t)). \tag{1}$$

where $\omega_n^2 = k_1/m$ and $\alpha = k_3/m$, while the saw-tooth like time-dependent time-delay $\tau(t)$ characterizes the sampling with sampling time h as shown in Fig. 1. The stability chart in Fig. 1 was identified by considering that the feedback is constant between sampling instants and it shows that the process experiences Hopf bifurcation along the red boundaries.

Hopf bifurcation analysis

For the bifurcation analysis of dynamical system (1) the concept of history functions is applied, which is usually considered for delay differential equations. Let us define the history functions

$$\boldsymbol{X}_j(\vartheta) = \begin{bmatrix} x_j(\vartheta) \\ v_j(\vartheta) \end{bmatrix}, \text{ where } x_j(\vartheta) = x(t_j+\vartheta),\ v_j(\vartheta) = \dot{x}(t_j+\vartheta),\ \vartheta \in [-h, 0],\ t_j = jh,\ j = 0, 1, 2\ldots \tag{2}$$

A nonlinear implicit mapping is created between subsequent history functions based on the equation of motion (1):

$$\boldsymbol{X}_{j+1}(\vartheta) = \boldsymbol{\Phi}_I(\boldsymbol{X}_j, \boldsymbol{X}_{j+1}, \vartheta) + \mathbf{f}(\boldsymbol{X}_{j+1}, \vartheta), \tag{3}$$

where the linear terms are included in the linear operator $\boldsymbol{\Phi}_I$, while the nonlinearities appear in the nonlinear operator $\mathbf{f}$:

$$\boldsymbol{\Phi}_I(\boldsymbol{X}_j, \boldsymbol{X}_{j+1}, \vartheta) = \begin{bmatrix} x_j(0) + v_j(0)(h+\vartheta) - \omega_n^2 \int_{-h}^{\vartheta}\int_{-h}^{s} x_{j+1}(r)\,dr\,ds + (1-P)\omega_n^2 x_j(-h)(\frac{1}{2}\vartheta^2 + h\vartheta + \frac{1}{2}h^2) \\ v_j(0) - \omega_n^2 \int_{-h}^{\vartheta} x_{j+1}(s)\,ds + (1-P)\omega_n^2 x_j(-h)(h+\vartheta) \end{bmatrix},$$

$$\mathbf{f}(\boldsymbol{X}_{j+1}, \vartheta) = \begin{bmatrix} -\alpha \int_{-h}^{\vartheta}\int_{-h}^{s} x_{j+1}^3(r)\,dr\,ds \\ -\alpha \int_{-h}^{\vartheta} x_{j+1}^3(s)\,ds \end{bmatrix}. \tag{4}$$

Equation (4) includes both the nonlinear effects and the sampling delay, however, the implicit terms make it difficult to handle this form. First, we apply a modal transformation. In order to find the necessary eigenfunctions, in generic cases, it is possible to formulate an explicit linear operator equivalent to $\boldsymbol{\Phi}_I$:

$$\boldsymbol{X}_{j+1}(\vartheta) = \boldsymbol{\Phi}_E \boldsymbol{X}_j(\vartheta), \quad \boldsymbol{\Phi}_E \boldsymbol{X}_j(\vartheta) = \begin{bmatrix} x_j(0)G_1(\vartheta) + x_j(-h)G_2(\vartheta) + v_j(0)G_3(\vartheta) \\ x_j(0)g_1(\vartheta) + x_j(-h)g_2(\vartheta) + v_j(0)g_3(\vartheta) \end{bmatrix}. \tag{5}$$

The functions $G_i(\vartheta)$ and $g_i(\vartheta)$ are calculated by solving the linearized equation of motion in closed form. The solutions of the explicit eigenvalue problem $\mu\mathbf{S}(\vartheta) = \mathbf{\Phi}_E\mathbf{S}(\vartheta)$ also solve the implicit one $\mu\mathbf{S}(\vartheta) = \mathbf{\Phi}_I(\mathbf{S}, \mu\mathbf{S}, \vartheta)$ and gives the same three characteristic multipliers $\mu_{1,2,3}$. Now let us define a scalar product over the space of the state functions by

$$\langle \mathbf{X}, \mathbf{Y} \rangle = \int_{-h}^{0} \mathbf{Y}^*(s)\mathbf{X}(s)\, ds,\ \mathbf{X}, \mathbf{Y} \in \mathbb{R} \to \mathbb{C}^2, \tag{6}$$

which makes the adjoint of the explicit operator $\mathbf{\Phi}_E$ take the form

$$\mathbf{\Phi}_E^* \begin{bmatrix} y_1(\vartheta) \\ y_2(\vartheta) \end{bmatrix} = \begin{bmatrix} \delta(\vartheta) \int_{-h}^{0} G_1^*(s)y_1(s) + g_1^*(s)y_2(s)\, ds + \delta(\vartheta + h) \int_{-h}^{0} G_2^*(s)y_1(s) + g_2^*(s)y_2(s)\, ds \\ \delta(\vartheta) \int_{-h}^{0} G_3^*(s)y_1(s) + g_3^*(s)y_2(s)\, ds \end{bmatrix}. \tag{7}$$

The adjoint eigenvalue problem $\mu\mathbf{N}(\vartheta) = \mathbf{\Phi}_E^*\mathbf{N}(\vartheta)$ presents the adjoint eigenfunctions. Scaling these adjoint eigenfunctions $\mathbf{N}_i$ such that $\langle \mathbf{S}_i, \mathbf{N}_i \rangle = 1$, we can define the modal coordinates

$$y_j = \langle \boldsymbol{X}_j, \mathbf{N}_1 \rangle,\ z_j = \langle \boldsymbol{X}_j, \mathbf{N}_2 \rangle,\ u_j = \langle \boldsymbol{X}_j, \mathbf{N}_3 \rangle,\ \text{and}\ \boldsymbol{w}_j(\vartheta) = \boldsymbol{X}_j(\vartheta) - y_j\mathbf{S}_1(\vartheta) - z_j\mathbf{S}_2(\vartheta) - u_j\mathbf{S}_3(\vartheta). \tag{8}$$

Projection of the implicit equation (3) with the adjoint eigenfunctions $\mathbf{N}_{1,2,3}(\vartheta)$ results in

$$\begin{aligned} \begin{bmatrix} y_{j+1} \\ z_{j+1} \\ u_{j+1} \end{bmatrix} &= \mathbf{B} \begin{bmatrix} y_{j+1} \\ z_{j+1} \\ u_{j+1} \end{bmatrix} + \mathbf{A} \begin{bmatrix} y_j \\ z_j \\ u_j \end{bmatrix} + \begin{bmatrix} \langle \mathbf{\Phi}_I(\boldsymbol{w}_j, \boldsymbol{w}_{j+1}) + \mathbf{f}(\boldsymbol{X}_{j+1}), \mathbf{N}_1 \rangle \\ \langle \mathbf{\Phi}_I(\boldsymbol{w}_j, \boldsymbol{w}_{j+1}) + \mathbf{f}(\boldsymbol{X}_{j+1}), \mathbf{N}_2 \rangle \\ \langle \mathbf{\Phi}_I(\boldsymbol{w}_j, \boldsymbol{w}_{j+1}) + \mathbf{f}(\boldsymbol{X}_{j+1}), \mathbf{N}_3 \rangle \end{bmatrix}, \\ \boldsymbol{w}_{j+1}(\vartheta) &= \mathbf{\Phi}_I(\boldsymbol{X}_j, \boldsymbol{X}_{j+1}, \vartheta) + \mathbf{f}(\boldsymbol{X}_{j+1}, \vartheta) - y_{j+1}\mathbf{S}_1(\vartheta) - z_{j+1}\mathbf{S}_2(\vartheta) - u_{j+1}\mathbf{S}_3(\vartheta), \end{aligned} \tag{9}$$

which can be rearranged linearly in an explicit way for y, z and u. At a Hopf bifurcation point, we can divide the function space into the center and stable subspaces. The center subspace is described by y and z with corresponding critical characteristic multipliers $\mu_{1,2} = e^{\pm i\beta}$, while u and $\boldsymbol{w}(\vartheta)$ are part of the stable subspace. The characteristic multiplier corresponding to mode u is $|\mu_3| < 1$, while $\mu_i = 0,\ i = 4, 5, \ldots$ because $\boldsymbol{w}(\vartheta)$ disappears from the linearized system entirely. According to the center manifold theorem, we may restrict the dynamics to the center manifold [3]. The approximation of the center manifold must be done up to third degree in $\boldsymbol{w}_j(\vartheta) = \boldsymbol{W}(y_j, z_j, \vartheta)$ and $u_j = U(y_j, z_j)$. Finally, by substituting the linearly explicit expression for y_{j+1} and z_{j+1} into the nonlinearities, we push the implicit terms to higher orders, thus, one obtains the explicit third order complex normal form of this Hopf bifurcation:

$$\begin{bmatrix} y_{j+1} \\ z_{j+1} \end{bmatrix} = \begin{bmatrix} \mu_1 & 0 \\ 0 & \mu_2 \end{bmatrix} \begin{bmatrix} y_j \\ z_j \end{bmatrix} + \begin{bmatrix} 1 & 0 & 0 \\ 0 & 1 & 0 \end{bmatrix} (\mathbf{I} - \mathbf{B})^{-1} \begin{bmatrix} \langle \mathbf{\Phi}_I(\boldsymbol{W}_j, \boldsymbol{W}_{j+1}) + \mathbf{f}(\mu_1 y_j\mathbf{S}_1 + \mu_2 z_j\mathbf{S}_2), \mathbf{N}_1 \rangle \\ \langle \mathbf{\Phi}_I(\boldsymbol{W}_j, \boldsymbol{W}_{j+1}) + \mathbf{f}(\mu_1 y_j\mathbf{S}_1 + \mu_2 z_j\mathbf{S}_2), \mathbf{N}_2 \rangle \\ \langle \mathbf{\Phi}_I(\boldsymbol{W}_j, \boldsymbol{W}_{j+1}) + \mathbf{f}(\mu_1 y_j\mathbf{S}_1 + \mu_2 z_j\mathbf{S}_2), \mathbf{N}_3 \rangle \end{bmatrix}. \tag{10}$$

The Hopf calculations made using normal form (10) are presented in Fig. 2 and compared to numerical simulations of equation (1). The calculations show good agreement with the numerical simulations.

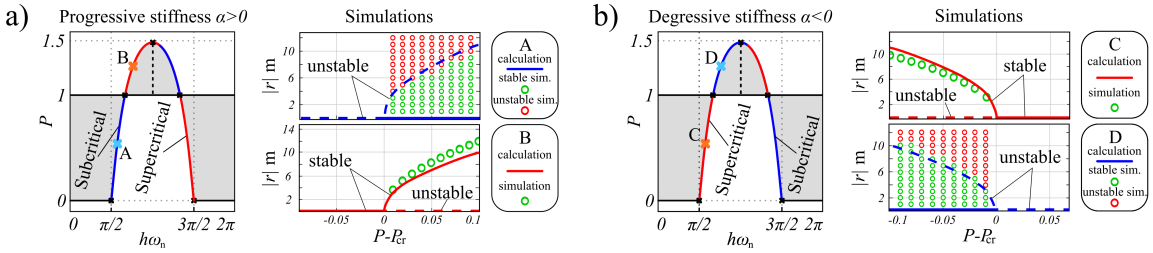

Figure 2: Bifurcation diagrams of the sampled nonlinear force control problem for $\omega_n = 100$ rad/s with progressive stiffness $\alpha = 10$ rad/sm^2 in panel a) and degressive stiffness $\alpha = -10$ rad/sm^2 in panel b).

Conclusions

A model of sampled force control on a single degree-of-freedom oscillator with nonlinear stiffness was investigated. Using the presented method, both sub- and supercritical Hopf-bifurcations were identified. Both types of bifurcations appeared for progressive and degressive stiffness characteristics, however, their locations are reversed in the two cases. The predicted limit-cycle amplitudes also match the ones obtained with numerical simulations.

References

[1] van de Wouw N., Nešić D., Heemels W.P.M.H. (2012) A discrete-time framework for stability analysis of nonlinear networked control systems. *Automatica* Volume 48, Issue 6

[2] Stepan G. (2001) Vibrations of machines subjected to digital force control. *International Journal of Solids and Structures* Volume 38, Issues 10–13

[3] Kuznetsov Y.A. (1998) Elements of Applied Bifurcation Theory Second Edition. Springer-Verlag New York, New York